

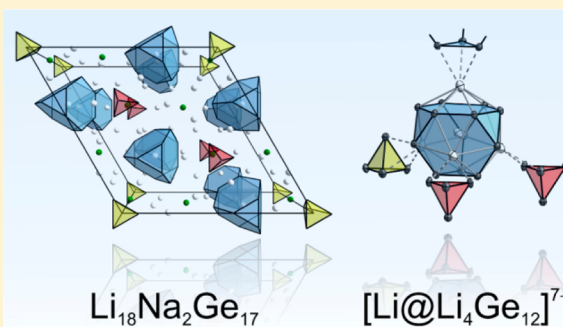
Li₁₈Na₂Ge₁₇—A Compound Demonstrating Cation Effects on Cluster Shapes and Crystal Packing in Ternary Zintl Phases

Lavinia M. Scherf, Michael Zeilinger, and Thomas F. Fässler*

Department Chemie, Technische Universität München, Lichtenbergstraße 4, 85747 Garching b. München, Germany

Supporting Information

ABSTRACT: The novel ternary Zintl phase Li₁₈Na₂Ge₁₇ was synthesized from a stoichiometric melt and characterized crystallographically. It crystallizes in the trigonal space group *P31m* (No. 157) with *a* = 17.0905(4) Å, *c* = 8.0783(2) Å, and *V* = 2043.43(8) Å³ (final *R* indices *R*₁ = 0.0212 and *wR*₂ = 0.0420 for all data). The structure contains three different Zintl anions in a 1:1:1 ratio: isolated anions Ge^{4−}, tetrahedra [Ge₄]^{4−}, and truncated, Li-centered tetrahedra [Li@Ge₁₂]^{11−}, whose hexagonal faces are capped by four Li cations, resulting in the Friauf polyhedra [Li@Li₄Ge₁₂]^{7−}. According to the Zintl–Klemm concept, Li₁₈Na₂Ge₁₇ is an electronically balanced Zintl phase, as experimentally verified by its diamagnetism. The compound is structurally related to Li₇RbGe₈, which also contains [Ge₄]^{4−} and [Li@Li₄Ge₁₂]^{7−} in its anionic substructure. However, exchanging the heavier alkali metal cation Rb for Na in the mixed-cation germanides leads to drastic changes in stoichiometry and crystal packing, demonstrating the great effects that cations exert on such Zintl phases through optimized cluster sheathing and space filling.



INTRODUCTION

Zintl phases are commonly defined as saltlike intermetallic compounds with highly heteropolar bonds. Formally, they can be described by a complete valence electron transfer from electropositive elements such as alkali or alkaline-earth metals to the more electronegative p-block metals of groups 13–16. Resulting Zintl anions typically behave like elements with the same number of valence electrons *N* according to the octet (*8* − *N*) rule.¹ Just like the corresponding elements, Zintl anions may take the form of extensive polymeric structures as well as few-atom clusters or isolated atoms. Ge cluster anions range from Br₂-like [Ge₂]^{6−} dumbbells in BaMg₂Ge₂² and P₄-analogous [Ge₄]^{4−} tetrahedra in A₄Ge₄ (*A* = Na, K, Rb, Cs)³ to truncated tetrahedra [Ge₁₂]^{12−} in Li₇RbGe₈.⁴ Some examples of such Ge Zintl anions are depicted in Figure 1. Isolated Ge^{4−} anions with noble-gas configurations are frequently observed as well: for example, in compounds E₂Ge (*E* = Mg, Ca, Sr, Ba).⁵ Examples of polymeric germanides are CaGe₂ (³∞[Ge[−]], As_{gray} structure),⁶ CaGe (¹∞[Ge^{2−}], polymeric Se structure),⁷ Li₇Ge₁₂ (²∞[Ge₂₄^{14−}]),⁸ and clathrate-type compounds Ba₆Ge₂₅,⁹ A_{*x*}Ge₄₆ (*A* = K, Rb, Cs, Ba),¹⁰ and A_{*x*}Ge₁₃₆ (*A* = Na, K, Rb).¹¹

The formation of the novel allotrope *m-allo*-Ge as a microcrystalline bulk material¹⁴ in a topotactic reaction of Li₇Ge₁₂ triggered our interest in looking for other allotropes of Ge and Si.¹⁵ In the course of our investigations, we considered Li₃NaSi₆ as a potential precursor because it has a two-dimensional Si substructure similar to that of Li₇Ge₁₂ and a topotactic conversion to *allo*-Si has been reported.¹⁶ During our attempts to synthesize a solid solution Li₃NaSi₆/Li₃NaGe₆ as a

precursor of a new modification of binary Si–Ge, we serendipitously obtained the new compound Li₁₈Na₂Ge₁₇.

A single-crystal X-ray structure determination shows that the novel Zintl phase Li₁₈Na₂Ge₁₇ contains the largest known anionic cluster unit, [Ge₁₂]^{12−}, which has been observed in only one other compound—the structurally related Li₇RbGe₈.⁴ Moreover, Li₁₈Na₂Ge₁₇ features three different Ge Zintl anions. Reports of compounds comprised of three or more different Zintl anions are extremely rare. The few examples include Ba₆Mg_{10.8}Li_{1.2}Si₁₂ (Si^{4−}, [Si₂]^{6−} dumbbells, bent [Si₃]^{7.4−} chains),¹⁷ E₃₁Sn₂₀ (*E* = Ca, Sr, Yb; Sn^{4−}, [Sn₂]^{6−} dumbbells, linear [Sn₅]^{12−} chains),¹⁸ Yb₃₆Sn₂₃ (Sn^{4−}, [Sn₂]^{6−} dumbbells, linear [Sn₆]^{14−} chains)¹⁹ and Na₂₃K₉Tl_{15.3} (Tl^{5−}, linear [Tl₃]^{7−} chains, [Tl₄]^{8−} tetrahedra, trigonal-bipyramidal [Tl₅]^{7−}).²⁰

Rather complex Zintl phases with various anions of different sizes require an equally complex and efficient coordination by cations. Corbett described the concepts and effects of this cluster “solvation” in detail.²¹ In short, surrounding cations stabilize anionic clusters by bridging and separating them. Stable Zintl phases require an optimized balance of specific cluster sheathing and efficient space filling. Interestingly, some Ge Zintl anions (e.g., [Ge₂]^{6−} in BaMg₂Ge₂,² [Ge₁₂]^{12−} in Li₇RbGe₈⁴) have only been obtained in ternary compounds with mixed cations. Others (e.g., [Ge₄–Na–Ge₄]^{7−} in A₇NaGe₈ with *A* = K, Rb)²² show packing schemes very different from those of their binary analogues. These examples along with extensive studies on mixed cation trielides performed by Dong

Received: October 27, 2013

Published: January 31, 2014

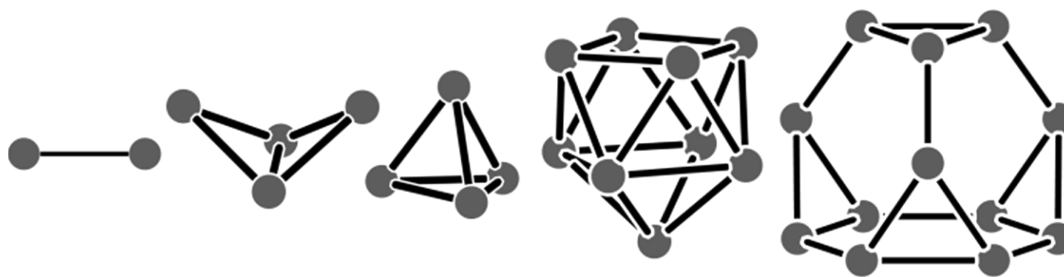


Figure 1. Selected Ge cluster anions from left to right: $[\text{Ge}_2]^{6-}$ dumbbell (BaMg_2Ge_2),² butterfly-shaped $[\text{Ge}_4]^{6-}$ ($\beta\text{-Ba}_3\text{Ge}_4$),¹² $[\text{Ge}_4]^{4-}$ tetrahedron (A_4Ge_4 ; A = Na, K, Rb, Cs),³ monocapped-quadratic-antiprismatic $[\text{Ge}_9]^{4-}$ (K_4Ge_9),¹³ truncated-tetrahedral $[\text{Ge}_{12}]^{12-}$ (Li_7RbGe_8).⁴

and Corbett^{20,23} demonstrated that mixing cations of different sizes can be a very useful tool for achieving this balance.²¹ Ab initio calculations on the structural differences in NaTl and KTI²⁴ as well as Li_2AuBi and Na_2AuBi ²⁵ support the frequently observed structure-directing effect of cations in Zintl compounds. The new Zintl phase $\text{Li}_{18}\text{Na}_2\text{Ge}_{17}$ presented here clearly illustrates the influence of cations on cluster shapes and crystal packing in ternary Zintl phases.

EXPERIMENTAL SECTION

Synthesis of $\text{Li}_{18}\text{Na}_2\text{Ge}_{17}$. All steps of synthesis and sample preparation were carried out in an Ar-filled glovebox (MBraun, H_2O level <0.1 ppm, O_2 level <0.1 ppm). $\text{Li}_{18}\text{Na}_2\text{Ge}_{17}$ was prepared from the pure elements (99% Li rods, Rockwood-Lithium; 99% Na rods, Chempur; 99.999% Ge pieces, Chempur) in a tantalum ampule. The sealed ampule containing the stoichiometric reaction mixture with a total mass of 1 g was placed inside a silica reaction container, which was then evacuated and heated to 750 °C for 1 h. The resulting melt was cooled at a rate of 0.5 °C min^{-1} to 300 °C, at which temperature annealing of the reaction product was allowed for 3 h.

Single-Crystal Structure Determination. Crystals of $\text{Li}_{18}\text{Na}_2\text{Ge}_{17}$ were selected in an Ar-filled glovebox and sealed in 0.3 mm glass capillaries. For the best specimen, intensity data were collected at 123 K using a Bruker AXS X-ray diffractometer equipped with a CCD detector (APEX II, κ -CCD), a rotating anode FR591 with Mo $K\alpha$ radiation ($\lambda = 0.71073$ Å), and a MONTEL optic monochromator. Data collection was controlled with the Bruker APEX software package.²⁶ Integration, data reduction, and absorption correction were performed with the SAINT²⁷ and SADABS²⁸ packages. The structure was solved with direct methods (SHELXS-97) and refined with full-matrix least squares on F^2 (SHELXL-97).²⁹ Details of the single-crystal data collection and refinement are given in Table 1. Further details on the crystal structure investigation may be obtained as Supporting Information (atomic coordinates and isotropic displacement parameters in Table S1, CIF file) and from Fachinformationszentrum Karlsruhe, 76344 Eggenstein-Leopoldshafen, Germany (fax (+49)7247-808-666; e-mail crysdata@fiz-karlsruhe.de; http://www.fiz-karlsruhe.de/request_for_deposited_data.html) on quoting the deposition number CSD-426692.

Powder X-ray Diffraction Analysis. A PXRD pattern of $\text{Li}_{18}\text{Na}_2\text{Ge}_{17}$ was recorded using a Stoe STADI P diffractometer equipped with a Ge(111) monochromator for Cu $K\alpha$ radiation ($\lambda = 1.54056$ Å) and a Dectris MYTHEN DCS 1K solid-state detector. A crystalline sample of a $\text{Li}_{18}\text{Na}_2\text{Ge}_{17}$ synthesis product was ground in an agate mortar and filled into a 0.3 mm glass capillary, which was then sealed. The sample was measured within a 2θ range of 5–89° (PSD steps, 0.075°; time/step, 45 s). The diffraction pattern is shown in Figure S2 in the Supporting Information.

Magnetic Measurements. Using a Quantum Design MPMS 5 XL SQUID magnetometer, the magnetization of 39 mg of a $\text{Li}_{18}\text{Na}_2\text{Ge}_{17}$ synthesis product was measured at applied fields of 5000 and 10000 Oe over the temperature range 2–300 K. The data were corrected for the sample holder and for ion-core diamagnetism using Pascal's constants.³⁰ The molar susceptibility X_m is negative in

Table 1. Crystallographic Data and Structure Refinement for $\text{Li}_{18}\text{Na}_2\text{Ge}_{17}$

<i>T</i> (K)	123(2)
formula wt	1404.93
cryst size (mm^3)	0.11 × 0.13 × 0.28
cryst color	metallic black
cryst shape	block
space group	$P31m$
unit cell dimens (Å)	
<i>a</i>	17.0905(4)
<i>c</i>	8.0783(2)
<i>Z</i>	3
<i>V</i> (Å ³)	2043.43(8)
ρ (calcd) (g cm^{-3})	3.425
μ (mm^{-1})	18.459
<i>F</i> (000)	1860
θ range (deg)	2.38–33.16
index range	–26 ≤ <i>h</i> ≤ 26 –25 ≤ <i>k</i> ≤ 23 –12 ≤ <i>l</i> ≤ 12
no. of rflns collected	47691
no. of indep rflns	5466 ($R_{\text{int}} = 0.0407$)
no. of rflns with $I > 2\sigma(I)$	5150 ($R_\sigma = 0.0250$)
abs cor	multiscan
no. of data/restraints/params	5466/1/191
goodness of fit on F^2	1.041
final <i>R</i> indices ($I > 2\sigma(I)$) ^{a,b}	
<i>R</i> 1	0.0185
<i>wR</i> 2	0.0412
<i>R</i> indices (all data) ^{a,b}	
<i>R</i> 1	0.0212
<i>wR</i> 2	0.0420
Flack param	0.01(2)
largest diff peak, hole (e \AA^{-3})	0.88, –0.99

$${}^a R1 = \sum |F_o| - |F_c| / \sum |F_o|, {}^b wR2 = [\sum w(F_o^2 - F_c^2)^2 / \sum w(F_o^2)^2]^{1/2}.$$

the range of $-(1.44\text{--}1.55) \times 10^{-3}$ emu mol^{-1} and temperature independent, as expected for a diamagnetic compound. The corresponding graph is shown in Figure S3 in the Supporting Information.

RESULTS AND DISCUSSION

Structure of $\text{Li}_{18}\text{Na}_2\text{Ge}_{17}$. $\text{Li}_{18}\text{Na}_2\text{Ge}_{17}$ was serendipitously identified from a reaction intended to yield $\text{Li}_3\text{NaSi}_3\text{Ge}_3$, a derivative of the known Zintl phase Li_3NaSi_6 .¹⁶ Subsequently, the air- and moisture-sensitive compound was synthesized directly from the pure elements and characterized crystallographically. $\text{Li}_{18}\text{Na}_2\text{Ge}_{17}$ crystallizes in the trigonal space group $P31m$ (No. 157) with $a = 17.0905(4)$ Å, $c = 8.0783(2)$ Å, and Z

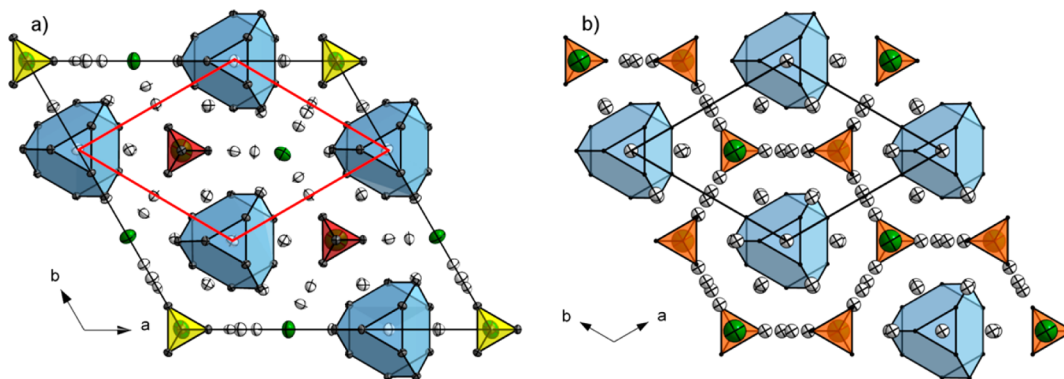


Figure 2. (a) Projection of the structure of $\text{Li}_{18}\text{Na}_2\text{Ge}_{17}$ onto the ab plane (Li, white; Na, green; Ge, gray; thermal ellipsoids at 90% probability at 123 K). The anionic Ge clusters are highlighted as colored polyhedra (truncated tetrahedra $[\text{Ge}_{12}]^{12-}$, blue; crystallographically different tetrahedra $[\text{Ge}_4]^{4-}$ (A) red, (B) yellow). The hexagonal primitive packing of truncated tetrahedra is indicated by red lines. (b) Projection of the structure of Li_7RbGe_8 onto the ab plane (Li, white; Rb, green; Ge, gray). The anionic Ge clusters are highlighted as colored polyhedra (truncated tetrahedra $[\text{Ge}_{12}]^{12-}$, blue; tetrahedra $[\text{Ge}_4]^{4-}$, orange).

= 3. All atoms were refined anisotropically with final reliability factors of $R1 = 0.0212$ and $wR2 = 0.0420$ for all data (Table 1).

Interestingly, the structure of $\text{Li}_{18}\text{Na}_2\text{Ge}_{17}$ incorporates three different Zintl anions in a 1:1:1 ratio: truncated Ge tetrahedra $[\text{Ge}_{12}]^{12-}$, Ge tetrahedra $[\text{Ge}_4]^{4-}$, and isolated Ge anions Ge^{4-} (Figure 2a). Thus, to the best of our knowledge, it is the first germanide containing three different Zintl anions with each of them observing the $(8 - N)$ rule. In addition, the new Zintl phase $\text{Li}_{18}\text{Na}_2\text{Ge}_{17}$ is only the second compound containing the largest known anionic Ge cluster unit, $[\text{Ge}_{12}]^{12-}$. Such $[\text{Ge}_{12}]^{12-}$ truncated tetrahedra have been reported once before in the related Zintl phase Li_7RbGe_8 , in which they occur next to tetrahedral $[\text{Ge}_4]^{4-}$.⁴ Similar $[\text{Sn}_{12}]^{12-}$ clusters are observed in $\text{ENa}_{10}\text{Sn}_{12}$ ($E = \text{Ca}, \text{Sr}$).³¹ Larger Ge polyanions have only been isolated via soluble $[\text{Ge}_9]^{4-}$, with $[\text{Ge}_{45}]^{12-}$ being the largest example of covalently linked Ge atoms.³²

The shape of the large $[\text{Ge}_{12}]^{12-}$ unit, a polyhedron with four triangular and four hexagonal faces, derives from a large tetrahedron with truncated vertices. Four Li atoms cap the hexagonal faces of the truncated tetrahedron and thus constitute the 16-vertex Friauf³³ polyhedron $[\text{Li}_4\text{Ge}_{12}]^{8-}$. In addition, the Friauf polyhedron is centered by one Li atom (Figure 3). Due to the lower crystal symmetry, Ge–Ge bond lengths (2.4840(5)–2.6948(5) Å) vary in a greater range than in Friauf polyhedra in Li_7RbGe_8 (2.505(2)–2.603(2) Å).⁴ However, average Ge–Ge bond lengths are identical (2.567(1) Å for $\text{Li}_{18}\text{Na}_2\text{Ge}_{17}$, 2.569(2) Å for Li_7RbGe_8). Similarly, the average interatomic distances of Ge and capping Li atoms (2.91(1) Å for $\text{Li}_{18}\text{Na}_2\text{Ge}_{17}$, 2.96(2) Å for Li_7RbGe_8) as well as the interatomic distances of centering Li1 to all 16 surrounding atoms (2.99(1) Å for $\text{Li}_{18}\text{Na}_2\text{Ge}_{17}$, 3.02(2) Å for Li_7RbGe_8) fall in the same ranges (Table 2). In addition, the Friauf polyhedron $[\text{Li}@\text{Li}_4\text{Ge}_{12}]^{7-}$ is coordinated by another 30 alkali-metal cations, forming an approximately spherical “solvation” environment (Figure S1 in the Supporting Information).

The four capping Li atoms link the Friauf polyhedron to neighboring Zintl anions (Figure 3). Li2 is coordinated by a triangular face of a neighboring Friauf polyhedron along c , whereas Li4 coordinates one edge of crystallographically distinguishable tetrahedra A and Li3 coordinates a face of the second tetrahedron type B.

Ge tetrahedra A and B (ratio 2:1) are both located on 3-fold rotation axes (Figure 2a) and differ in their relative orientations

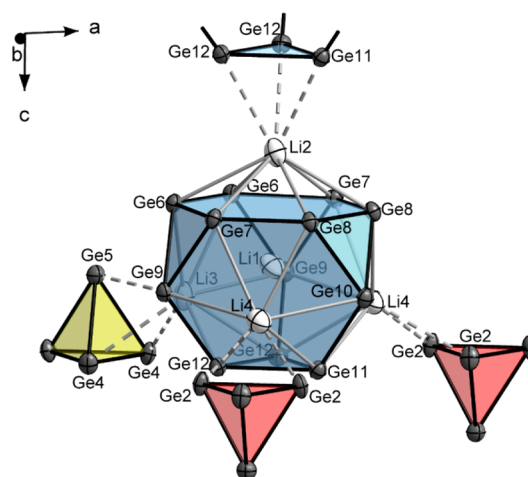


Figure 3. Structure of the Li-centered Friauf polyhedron $[\text{Li}@\text{Li}_4\text{Ge}_{12}]^{7-}$ (Li, white; Ge, gray; truncated tetrahedron $[\text{Ge}_{12}]^{12-}$, blue; crystallographically different tetrahedra $[\text{Ge}_4]^{4-}$ (A) red, (B) yellow; thermal ellipsoids at 90% probability at 123 K). Ge–Ge bonds are marked in black, whereas capping Li atoms are connected with gray lines. Interactions of capping Li atoms with edges (A) or triangular faces (B and $[\text{Li}@\text{Li}_4\text{Ge}_{12}]^{7-}$) of neighboring clusters are shown with broken lines. Relevant interatomic distances are given in Table 2.

as well as their coordination environments (Figure 4a,b). Nevertheless, their Ge–Ge bond lengths of 2.5610(5)–2.5818(6) Å agree well with those in A_4Ge_4 ($A = \text{Na}, \text{K}, \text{Rb}, \text{Cs}$).³ Tetrahedron A has a coordination environment similar to that of $[\text{Ge}_4]^{4-}$ tetrahedra in Li_7RbGe_8 ,⁴ containing 12 Li and 2 Na atoms (Figure 4a; Ge–Li distances 2.575(5)–3.114(6) Å, Ge–Na distances 2.980(2)–3.320(2) Å). In contrast, tetrahedron B is coordinated by 15 Li and 2 Na atoms (Figure 4b; Ge–Li distances 2.703(7)–3.095(6) Å, Ge–Na distances 3.020(3)–3.335(2) Å). For both tetrahedron types, Li atoms cap trigonal faces or bridge edges or coordinate *exo* at vertices. These coordination modes commonly occur in Zintl cluster sheathing.²¹

The isolated Ge atom Ge1 is coordinated by nine Li atoms and Na1 (Figure 4c) with a Ge–Na distance of 2.877(2) Å. Coordinating Li atoms (Ge–Li distance 2.514(6)–2.903(5) Å) are clearly differentiated from next-nearest neighbors with Ge–Li distances >4.8 Å. All relevant interatomic distances in $\text{Li}_{18}\text{Na}_2\text{Ge}_{17}$ are given in Table 2.

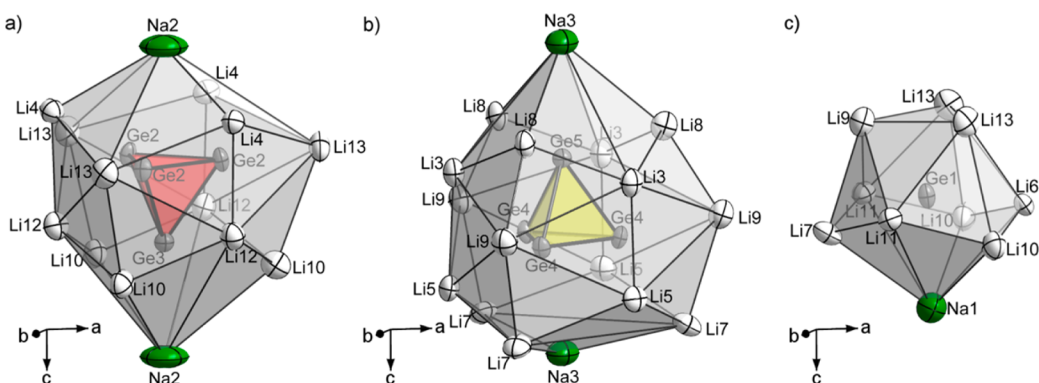


Figure 4. Coordination environments of (a) the Ge tetrahedron A, (b) the Ge tetrahedron B, (c) and the isolated Ge atom Ge1 (Li, white; Na, green; Ge, gray; thermal ellipsoids at 90% probability at 123 K). Relevant interatomic distances are given in Table 2.

Table 2. Relevant Interatomic Distances in $\text{Li}_{18}\text{Na}_2\text{Ge}_{17}$ ($P31m$, $Z = 3$, Estimated Standard Deviations in Parentheses)

atom pair		d (Å)	atom pair		d (Å)	atom pair		d (Å)
Ge1	Li6	2.514(6)	Ge6	Ge6	2.4883(5)	Ge9	Li8	2.856(4)
	Li11 \times 2	2.543(5)		Ge9	2.5980(4)		Li13	2.921(5)
	Li9	2.560(7)		Ge7	2.6596(4)		Li3	2.935(3)
	Li13 \times 2	2.643(5)		Li11	2.708(4)		Li4	2.978(4)
	Li7	2.709(7)		Li7	2.740(3)		Li1	3.058(3)
	Na1	2.877(2)		Li8	2.752(3)		Na1	3.161(1)
	Li10 \times 2	2.902(5)		Li5	2.836(6)		Ge10	Ge11
Ge2	Ge2 \times 2	2.5610(5)	Li3	2.906(6)	Ge8 \times 2	2.5596(4)		
	Ge3	2.5753(4)	Li2	2.974(6)	Li13 \times 2	2.826(5)		
	Li13	2.575(5)	Li1	2.995(6)	Li4 \times 2	2.946(4)		
	Li4	2.854(5)	Ge7	Ge8	2.4952(4)	Na1	2.978(2)	
	Li4	2.885(5)		Ge9	2.5651(4)	Li1	3.042(6)	
	Li12	2.924(5)	Li11	2.618(5)	Ge11	Ge10	2.4839(5)	
	Li12	2.932(5)	Ge6	2.6596(4)		Li6	2.585(6)	
	Li10	3.114(6)	Li10	2.767(5)	Ge12 \times 2	2.5921(4)		
Na2	3.335(2)	Li4	2.882(5)	Li4 \times 2	2.871(5)			
Ge3	Ge2 \times 3	2.5753(4)	Li12	2.951(6)	Li12 \times 2	2.903(5)		
	Li12 \times 3	2.862(5)	Li2	2.980(4)	Li2	2.960(8)		
	Li10 \times 3	2.975(6)	Li1	2.997(4)	Li1	2.964(7)		
	Na2	2.980(2)	Ge8	Ge7	2.4952(4)	Ge12	Ge9	2.5000(4)
Ge4	Ge5	2.5688(6)		Ge10	2.5597(4)		Li11	2.567(5)
	Ge4 \times 2	2.5818(6)	Li6	2.659(5)	Ge11	2.5921(4)		
	Li9	2.703(7)	Ge8	2.6948(5)	Ge12	2.5992(5)		
	Li5 \times 2	2.823(6)	Li10	2.768(5)	Li5	2.766(6)		
	Li7	2.902(7)	Li4	2.851(5)	Li4	2.857(5)		
	Li3 \times 2	3.035(6)	Li12	2.912(6)	Li3	2.875(6)		
	Li8	3.095(6)	Li2	2.916(6)	Li12	2.942(5)		
	Na3	3.320(2)	Li1	2.969(6)	Li1	2.945(7)		
Ge5	Ge4 \times 3	2.5688(6)	Ge9	Ge12	2.5000(4)	Li2	3.018(7)	
	Li8 \times 3	2.770(6)		Ge7	2.5651(4)	Li2	2.94(1)	
	Li3 \times 3	2.838(6)	Ge6	2.5980(4)	Li3	2.981(9)		
	Na3	3.020(3)	Li9	2.855(4)	Li4 \times 2	3.009(6)		
					Li1			

Electron Count. According to the Zintl–Klemm concept,^{1a,34} the truncated Ge tetrahedron may be viewed as a $[\text{Ge}_{12}]^{12-}$ anion with one negative charge for every three-connected Ge atom. Adding the four capping Li atoms and Li1 in the center with one positive charge each results in an overall electron count of -7 for $[\text{Li}@\text{Li}_4\text{Ge}_{12}]^{7-}$. $\text{Li}_{18}\text{Na}_2\text{Ge}_{17}$ contains the Friauf polyhedron, tetrahedral $[\text{Ge}_4]^{4-}$, and isolated Ge^{4-} in a 1:1:1 ratio. Thus, $(\text{Li}^+)_{13}(\text{Na}^+)_2[\text{Li}@\text{Li}_4\text{Ge}_{12}]^{7-}[\text{Ge}_4]^{4-}(\text{Ge}^{4-})$ is an appropriate notation for this novel Zintl phase, in which all Zintl anions obey the $(8 - N)$

rule. A magnetic measurement of $\text{Li}_{18}\text{Na}_2\text{Ge}_{17}$ clearly reveals diamagnetism of the metallic black and brittle compound (Figure S3 in the Supporting Information), which is consistent with a semiconducting Zintl phase.

Cation Effects. The crystal structure of $\text{Li}_{18}\text{Na}_2\text{Ge}_{17}$ is closely related to the structure of Li_7RbGe_8 .⁴ In both compounds, the Li-centered Friauf polyhedra $[\text{Li}@\text{Li}_4\text{Ge}_{12}]^{7-}$ arrange in a hexagonally primitive fashion, as demonstrated in Figure 2. The resulting voids are filled by $[\text{Ge}_4]^{4-}$ tetrahedra and in the case of $\text{Li}_{18}\text{Na}_2\text{Ge}_{17}$ also by isolated Ge anions.

Alkali-metal cations Li^+ as well as Na^+ and Rb^+ , respectively, stabilize the Zintl anions by counterbalancing the negative charge, filling voids and providing cluster sheathing that keeps clusters separated.

Although the heavier alkali-metal content in the two ternary germanides only amounts to 5.41 ($\text{Li}_{18}\text{Na}_2\text{Ge}_{17}$) and 6.25 atom % (Li_7RbGe_8), the exchange of the heavier alkali-metal cation induces a dramatic difference in the crystal structures. A comparison of cell dimensions of the hexagonally primitive framework of Friauf polyhedra in both compounds shows a slight cell contraction upon utilization of Na instead of Rb (Table 3), changing the requirements for effective space filling.

Table 3. Cell Dimensions a' , c' , and V' of the Hexagonally Primitive Friauf Polyhedron Framework in $\text{Li}_{18}\text{Na}_2\text{Ge}_{17}$ (Room-Temperature Powder Data; $a' = (1/3)^{1/2}a$; $c' = c$; $V' = (1/3)^{1/2}V$) and Li_7RbGe_8 (Room-Temperature Single-Crystal Data; $a' = a$; $c' = (1/2)c$; $V' = (1/2)V$)

	$\text{Li}_{18}\text{Na}_2\text{Ge}_{17}$	Li_7RbGe_8
a' (Å)	9.899(2)	9.8946(7)
c' (Å)	8.100(1)	8.135(2)
V' (Å ³)	679.74(4)	689.74(2)

An isolated Ge^{4-} anion replaces one of the two $[\text{Ge}_4]^{4-}$ tetrahedra in each primitive cell. However, the isolated anion, which has the same 4-fold negative charge as the larger $[\text{Ge}_4]^{4-}$ tetrahedron, cannot encompass the same number of cations in its coordination environment. Therefore, $[\text{Ge}_4]^{4-}$ tetrahedron **B** accommodates three additional Li cations, resulting in decreased overall symmetry and a greater a parameter. The lowered symmetry is accompanied by a slight distortion of the hexagonally primitive Friauf polyhedron framework in $\text{Li}_{18}\text{Na}_2\text{Ge}_{17}$. Whereas the distances of one Friauf polyhedron center to the centers of each of the six neighboring polyhedra in the ab plane are all equal in Li_7RbGe_8 (9.8946(7) Å, room-temperature single-crystal data), these center-to-center distances slightly differ in $\text{Li}_{18}\text{Na}_2\text{Ge}_{17}$ ($4 \times 9.931(6)$ Å, $2 \times 9.742(6)$ Å, 123 K single-crystal data).

In addition, the introduction of Na as the heavier alkali-metal cation evokes a drastic change of the crystal packing along the c direction (Figure 5). In Li_7RbGe_8 , two $[\text{Ge}_4]^{4-}$ tetrahedra are separated by two Rb cations and Friauf polyhedra are staggered due to a 6_3 screw axis. However, in $\text{Li}_{18}\text{Na}_2\text{Ge}_{17}$ a single Na cation alternates with each tetrahedron and isolated Ge anion, respectively. Concomitantly, the length of the c axis is halved (Table 3) because $[\text{Li}@\text{Li}_4\text{Ge}_{12}]^{7-}$ clusters stack in an eclipsed manner in the lower symmetry.

CONCLUSIONS

Mixing cations of different size or even different charge in syntheses of Zintl phases has been shown to be an efficient tool to stabilize rare cluster shapes. The novel compound $\text{Li}_{18}\text{Na}_2\text{Ge}_{17}$ presented here and the related Li_7RbGe_8 illustrate this concept well. Although the heavier alkali-metal content only amounts to 5–6 atom % in these compounds, the exchange of Rb by Na introduces a dramatic structural difference. In the case of $\text{Li}_{18}\text{Na}_2\text{Ge}_{17}$ an intriguing structure with three different Zintl anions is obtained. It is therefore easy to imagine that many more novel structures may be stabilized as mixed-cation compounds which are not available in binary systems. Thus, cation ratios must be carefully selected in order to obtain electronically balanced structures with favorable cluster sheathing and efficient space filling. However, owing to the multitude of Zintl anion geometries and countless possible combinations thereof, predicting new ternary Zintl phases remains difficult.

ASSOCIATED CONTENT

Supporting Information

Atomic coordinates and isotropic displacement parameters of $\text{Li}_{18}\text{Na}_2\text{Ge}_{17}$ (Table S1), coordination environment of the Friauf polyhedron $[\text{Li}@\text{Li}_4\text{Ge}_{12}]^{7-}$ in $\text{Li}_{18}\text{Na}_2\text{Ge}_{17}$ (Figure S1), a powder X-ray diffraction pattern of $\text{Li}_{18}\text{Na}_2\text{Ge}_{17}$ (Figure S2), results of magnetic susceptibility measurements (Figure S3), and a CIF file giving crystallographic data. This material is available free of charge via the Internet at <http://pubs.acs.org>.

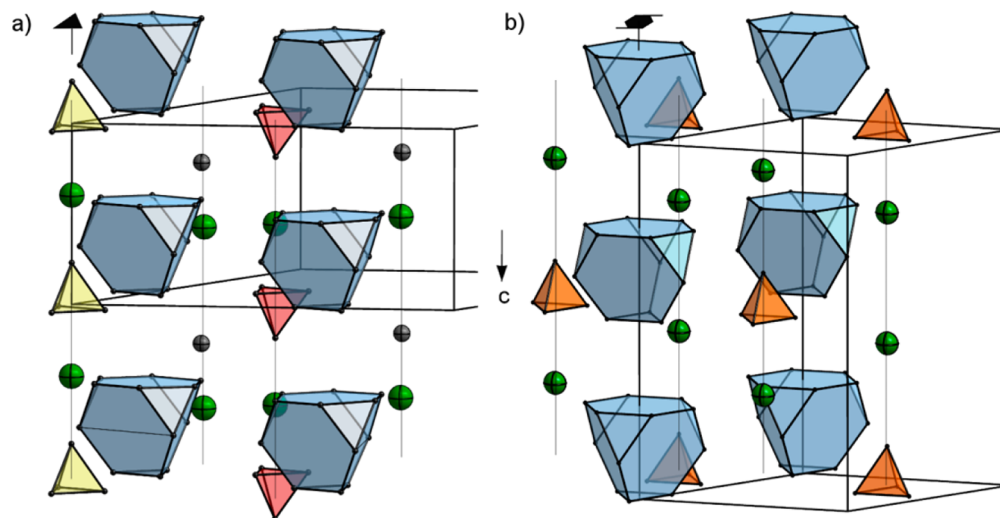


Figure 5. Fragments of the structures of (a) $\text{Li}_{18}\text{Na}_2\text{Ge}_{17}$ (Na, green; Ge, gray; truncated tetrahedra $[\text{Ge}_{12}]^{12-}$, blue; crystallographically different tetrahedra $[\text{Ge}_4]^{4-}$ (A) red, (B) yellow) and (b) Li_7RbGe_8 (Rb, green; Ge, gray; truncated tetrahedra $[\text{Ge}_{12}]^{12-}$, blue; tetrahedra $[\text{Ge}_4]^{4-}$, orange), demonstrating the packing of Zintl anions and Na and Rb cations, respectively, along c . The main symmetry elements are indicated by their symbols. Li atoms are omitted for enhanced clarity.

■ AUTHOR INFORMATION

Corresponding Author

*E-mail for T.F.F.: thomas.faessler@lrz.tum.de.

Notes

The authors declare no competing financial interest.

■ ACKNOWLEDGMENTS

The authors thank A. V. Hoffmann for the SQUID measurement and for financial support from the SolTech (Solar Technologies go Hybrid) program of the State of Bavaria. L.M.S. is further grateful to the Studienstiftung des Deutschen Volkes for her fellowship.

■ REFERENCES

- (1) (a) Zintl, E. *Angew. Chem.* **1939**, *52*, 1–6. (b) *Zintl Phases: Principles and Recent Developments*; Fässler, T. F., Ed.; Springer-Verlag: Heidelberg, Germany, 2011; Structure and Bonding Vol. 139.
- (2) (a) Eisenmann, B.; May, N.; Müller, W.; Schäfer, H.; Weiss, A.; Winter, J.; Ziegler, G. *Z. Naturforsch., B* **1970**, *25*, 1350–1352. (b) Eisenmann, B.; Schäfer, H. *Z. Anorg. Allg. Chem.* **1974**, *403*, 163–172.
- (3) (a) Witte, J.; von Schnering, H. G.; Klemm, W. *Z. Anorg. Allg. Chem.* **1964**, *327*, 260–273. (b) Busmann, E. *Z. Anorg. Allg. Chem.* **1961**, *313*, 90–106.
- (4) Bobev, S.; Sevov, S. C. *Angew. Chem.* **2001**, *113*, 1555–1558; *Angew. Chem., Int. Ed.* **2001**, *40*, 1507–1510.
- (5) (a) Zintl, E.; Kaiser, H. *Z. Anorg. Allg. Chem.* **1933**, *211*, 113–131. (b) Eckerlin, P.; Wölfel, E. *Z. Anorg. Allg. Chem.* **1955**, *280*, 321–331. (c) Eisenmann, B.; Schäfer, H.; Turban, K. *Z. Naturforsch., B* **1975**, *30*, 677–680. (d) Turban, K.; Schäfer, H. *Z. Naturforsch., B* **1973**, *28*, 220–222.
- (6) (a) Wallbaum, H. J. *Naturwissenschaften* **1944**, *32*, 76. (b) Tobash, P. H.; Bobev, S. *J. Solid State Chem.* **2007**, *180*, 1575–1581.
- (7) Eckerlin, P.; Meyer, H. J.; Wölfel, E. *Z. Anorg. Allg. Chem.* **1955**, *281*, 322–328.
- (8) (a) Kiefer, F.; Fässler, T. F. *Solid State Sci.* **2011**, *13*, 636–640. (b) Grüttner, A.; Nesper, R.; von Schnering, H. G. *Angew. Chem.* **1982**, *94*, 933; *Angew. Chem., Int. Ed. Engl.* **1982**, *21*, 912–913.
- (9) (a) Fukuoka, H.; Iwai, K.; Yamanaka, S.; Abe, H.; Yoza, K.; Häming, L. *J. Solid State Chem.* **2000**, *151*, 117–121. (b) Kim, S.-J.; Hu, S.; Uher, C.; Hogan, T.; Huang, B.; Corbett, J. D.; Kanatzidis, M. G. *J. Solid State Chem.* **2000**, *153*, 321–329. (c) Carrillo-Cabrera, W.; Curda, J.; von Schnering, H. G.; Paschen, S.; Grin, Y. *Z. Kristallogr.-New Cryst. Struct.* **2000**, *215*, 207–208.
- (10) (a) Cros, C.; Pouchard, M.; Hagemüller, P. *J. Solid State Chem.* **1970**, *2*, 570–581. (b) Liang, Y.; Böhme, B.; Ormeci, A.; Borrmann, H.; Pecher, O.; Haarmann, F.; Schnelle, W.; Baitinger, M.; Grin, Y. *Chem. Eur. J.* **2012**, *18*, 9818–9822. (c) Veremchuk, I.; Wosylus, A.; Böhme, B.; Baitinger, M.; Borrmann, H.; Prots, Y.; Burkhardt, U.; Schwarz, U.; Grin, Y. *Z. Anorg. Allg. Chem.* **2011**, *637*, 1281–1286.
- (11) (a) Simon, P.; Tang, Z.; Carrillo-Cabrera, W.; Chiong, K.; Böhme, B.; Baitinger, M.; Lichte, H.; Grin, Y.; Guloy, A. M. *J. Am. Chem. Soc.* **2011**, *133*, 7596–7601. (b) Bobev, S.; Sevov, S. C. *J. Am. Chem. Soc.* **1999**, *121*, 3795–3796.
- (12) Zürcher, F.; Nesper, R. *Angew. Chem.* **1998**, *110*, 3451–3454; *Angew. Chem., Int. Ed.* **1998**, *37*, 3314–3318.
- (13) Ponou, S.; Fässler, T. F. *Z. Anorg. Allg. Chem.* **2007**, *633*, 393–397.
- (14) Kiefer, F.; Karttunen, A. J.; Döblinger, M.; Fässler, T. F. *Chem. Mater.* **2011**, *23*, 4578–4586.
- (15) (a) Karttunen, A. J.; Fässler, T. F.; Linnolahti, M.; Pakkanen, T. *A. Inorg. Chem.* **2011**, *50*, 1733–1742. (b) Karttunen, A. J.; Fässler, T. F. *ChemPhysChem* **2013**, *14*, 1807–1817.
- (16) von Schnering, H. G.; Schwarz, M.; Nesper, R. *J. Less-Common Met.* **1988**, *137*, 297–310.
- (17) Wengert, S.; Nesper, R. *Z. Anorg. Allg. Chem.* **2000**, *626*, 246–252.
- (18) Ganguli, A. K.; Guloy, A. M.; Leon-Escamilla, E. A.; Corbett, J. D. *Inorg. Chem.* **1993**, *32*, 4349–4353.
- (19) Leon-Escamilla, E. A.; Corbett, J. D. *Inorg. Chem.* **1999**, *38*, 738–743.
- (20) Dong, Z.-C.; Corbett, J. D. *Inorg. Chem.* **1996**, *35*, 3107–3112.
- (21) Corbett, J. D. *Struct. Bonding (Berlin)* **1997**, *87*, 157–194.
- (b) Corbett, J. D. *Angew. Chem.* **2000**, *112*, 682–704; *Angew. Chem., Int. Ed.* **2000**, *39*, 670–690.
- (22) Llanos, J.; Nesper, R.; von Schnering, H. G. *Angew. Chem.* **1983**, *95*, 1026–1027; *Angew. Chem., Int. Ed. Engl.* **1983**, *22*, 998.
- (23) (a) Dong, Z.-C.; Corbett, J. D. *J. Am. Chem. Soc.* **1994**, *116*, 3429–3435. (b) Dong, Z. C.; Corbett, J. D. *J. Am. Chem. Soc.* **1995**, *117*, 6447–6455. (c) Cordier, G.; Müller, V. *Z. Naturforsch., B* **1994**, *49*, 935–938.
- (24) Wang, F.; Miller, G. J. *Inorg. Chem.* **2011**, *50*, 7625–7636.
- (25) Wang, F.; Miller, G. J. *Eur. J. Inorg. Chem.* **2011**, *2011*, 3989–3998.
- (26) APEX 2: APEX Suite of Crystallographic Software, 2008.4; Bruker AXS Inc., Madison, WI, USA, 2008.
- (27) SAINT; Bruker AXS Inc., Madison, WI, USA, 2001.
- (28) SADABS; Bruker AXS Inc., Madison, WI, USA, 2001.
- (29) Sheldrick, G. M. *Acta Crystallogr.* **2008**, *A64*, 112–122.
- (30) Bain, G. A.; Berry, J. F. *J. Chem. Educ.* **2008**, *85*, 532–536.
- (31) Bobev, S.; Sevov, S. C. *Inorg. Chem.* **2001**, *40*, 5361–5364.
- (32) (a) Scharfe, S.; Kraus, F.; Stegmaier, S.; Schier, A.; Fässler, T. F. *Angew. Chem.* **2011**, *123*, 3712–3754; *Angew. Chem., Int. Ed.* **2011**, *50*, 3630–3670. (b) Spiekermann, A.; Hoffmann, S. D.; Fässler, T. F.; Krossing, I.; Preiss, U. *Angew. Chem.* **2007**, *119*, 5404–5407; *Angew. Chem., Int. Ed.* **2007**, *46*, 5310–5313.
- (33) Friauf, J. B. *J. Am. Chem. Soc.* **1927**, *49*, 3107–3114.
- (34) (a) Klemm, W. *Proc. Chem. Soc.* **1958**, 329–341. (b) Klemm, W.; Busmann, E. *Z. Anorg. Allg. Chem.* **1963**, *319*, 297–311.